Journal of Structural Geology, Vol. 14, No. 8/9, pp. 953 to 962, 1992
Printed in Great Britain

0191-8141/92 $05.00+0.00

Finite element modelling of the propagation of a pressure solution cleavage seam

F. FUETEN

Department of Geological Sciences, Brock University, St. Catharines, Ontario, Canada L2S 3A1

and

P.-Y. F. ROBIN

Department of Geology, Erindale Campus, University of Toronto, Ontario, Canada L5L 1C6

(*Received* 6 *September* 1991; *accepted in revised form* 29 *March* 1992)

Abstract—The propagation of a cleavage seam is modelled by a two-dimensional finite element technique, which extends Fletcher and Pollard's elastic 'anticrack' theory to a composition-dependent viscous rheology. The viscous solution is obtained by repeated solutions of the force equilibrium equations at successive time steps, with the viscosity of each element varying as a function of its strain history. The rheology assumed follows previous modelling by Robin: the rock is modelled as a 'quartz'–'mica' mixture in which deformation proceeds by diffusion of 'silica'. The viscosity of an element depends on its proportion of 'quartz', varying from a minimum for intermediate 'quartz'–'mica' mixtures to higher values for either pure 'quartz' or pure 'micas'. As a result of its incremental strain, an element either loses or gains 'quartz' (i.e. volume), and therefore changes its viscosity for the next strain increment. The system can be either open ('silica' escapes the system; all individual elements lose volume) or closed (individual elements may gain or lose volume but the total volume of the system is preserved).

At the start of a run, a nucleus of a cleavage seam is introduced as a thin layer of elements with a lower viscosity (corresponding to a higher 'mica' content) than the rest of the rock. The stress concentration at the tip of the seam leads to a weakening of the elements in front of it through loss of 'quartz'; this results in crack propagation, for both open and closed systems. All other parameters being equal, the 'speed' of propagation is greater for open systems than for closed ones.

INTRODUCTION

SPACED cleavages of tectonic origin have been observed and studied in rocks for more than 100 years (Sorby 1863), and 'pressure solution'* is commonly believed to be an important part of the process leading to their development. However, many aspects of spaced cleavage formation remain enigmatic. We know little, for example, about the rate of the process under geological conditions, the parameters which determine cleavage spacing and cleavage morphology, the resulting rheological behaviour of a polymineralic rock deforming by pressure solution. Experimental work has not reproduced spaced pressure solution cleavage, perhaps because of the long time required in nature for detectable diffusion transfer. The present study is concerned with modelling the propagation of one pressure solution cleavage seam in rock which deforms by stress-induced diffusion transfer. It is an extension of the *anticrack* model of Fletcher & Pollard (1981), taking into account a composition-dependent rheology such as proposed by Robin (1979) and the possible transfer through the rock of at least one chemical component such as discussed by Fletcher (1982).

Fletcher & Pollard (1981) have pointed out that the cleavage seam could be viewed as a propagating *anticrack*: the compressive stress concentration at the tip of this anticrack is responsible for dissolution of material and consequent propagation of the cleavage. In order to model the stress concentration at the anticrack tip, Fletcher & Pollard (1981) assumed that the rock behaves elastically, except along the crack itself where pressure solution occurred. Pressure solution along the anticrack was modelled by taking the pressure to be zero along its walls. This implies instant and totally effective pressure solution along the walls of the anticrack; mechanically, the cleavage seam thus remains a 'hole' throughout the deformation. With these two assumptions, these authors can, by changing the signs, apply the results of elastic crack theory. As Fletcher & Pollard (1981) argue, an elastic material, with exclusive localization of pressure solution along discrete seams, appears to be an adequate model to describe stylolite evolution in shallowly deformed rocks. But pelitic rocks which deform, and develop a cleavage, under mesozonal metamorphic con-

*Pressure solution, a geological term, describes a class of deformation mechanisms in rocks which could be more accurately called *stress-induced diffusion transfer*. In metals and ceramics, stress-induced diffusion transfer is mainly called *Nabarro–Herring creep*, and *Coble creep*, two end-member models. Unlike in Nabarro–Herring creep and Coble creep, the polymineralic nature of a rock plays an important role in the observation of the phenomenon; the different and contrasting mobilities of the various chemical components, and the possibility of metamorphic reactions, also affect the process and its observation. Finally, the 'humidity' prevalent under the conditions of deformation in the Earth's crust is widely believed to influence the state of the grain boundaries along which diffusion proceeds and to catalyse the transfer mechanisms. In order to distinguish what happens in rocks from what happens in artificial materials, the traditional name of pressure solution is retained.

ditions are not well modelled by anticracks, because: (1) the cleavage seams, rather than being discrete and negligibly thin surfaces, may make up a significant volume fraction of the rock; and (2) pressure solution is likely to be an important deformation mechanism throughout the rock, not just along thin (or thick) cleavages.

We present here a model which does describe the propagation of a cleavage seam of finite thickness within a viscous rock deforming by pressure solution. The rock is modelled as a 'quartz'–'mica' mixture in which the deformation proceeds in significant part by diffusion of 'silica'. The viscosity of a small volume of rock depends on its modal proportions and varies during deformation. The model is *self-consistent* in that the changes in pressure near the cleavage surface are calculated consequences of an assumed composition-dependent viscosity and of the strain history, and thus need not be imposed separately.

The heterogeneous deformation associated with the propagation of the cleavage seam is modelled numerically by a finite element technique in which a 'small volume of rock' is represented by an *element*. An *element* is small enough for the assumptions of uniform stress and strain within it to be acceptable, and it therefore has a uniform viscosity. But an element is also large enough compared to the mineral grains constituting the rock to be assigned a meaningful and continuously variable modal mineral composition. The evolution with time of the cleavage seam is achieved by iterations of the finite element program which allow the individual elements to change their viscosities throughout the deformation.

COMPOSITION-DEPENDENT VISCOSITY

A dependence of the rheological properties of a homogeneous volume of rock on its composition is a basic fact of geology. For a rock exhibiting a cleavage, one would expect different rheological behaviours for cleavage and lithons. For their anticrack model of pressure solution, Fletcher & Pollard (1981) assume an extreme rheological dependence: a rock is elastic and strong outside of the seam, but it 'collapses', i.e. loses all strength, along the seam. In contrast, Robin (1979) noted that a creep strength which varies continuously with the modal composition of the rock: (1) was consistent with abundant petrographic observations of competency contrasts in rocks; (2) could account for the development of tectonic segregation layering; and (3) would be expected in rocks deforming by pressure solution of one mineral, e.g. quartz, if that pressure solution was somehow enhanced by the presence of another mineral, e.g. clay minerals, or micas. As pointed out by Robin (1979), silica mobility may simply be enhanced by easier diffusion through the phyllosilicate structures, or along cleavage planes lined with adsorbed H_2O. Petrographic observations, the earliest being those of Heald (1956) on pressure solution between grains, are themselves strong arguments for such a catalytic action of phyllosilicates.

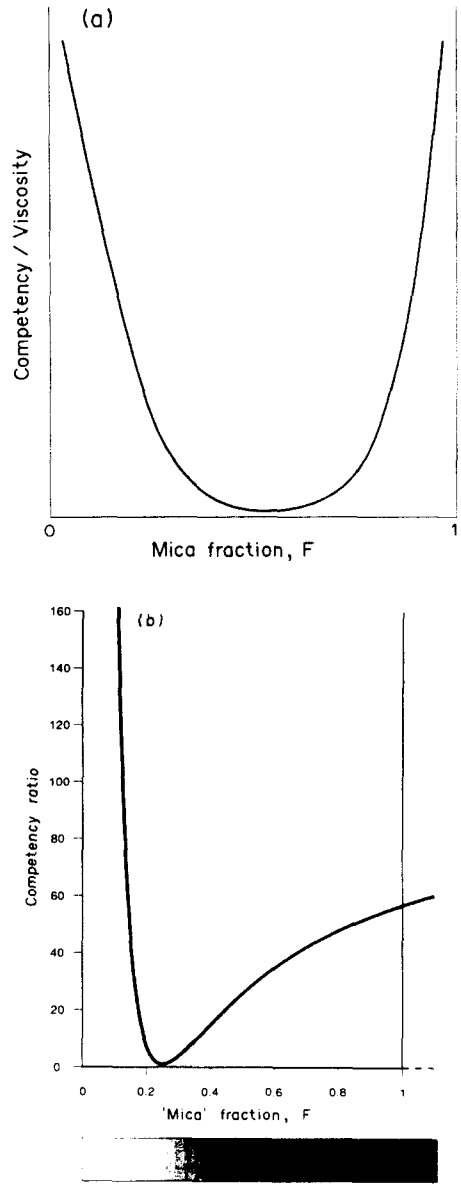

Fig. 1. (a) Dependence of viscosity on modal 'mica' fraction, F (after Robin 1979, fig. 1); (b) dependence of viscosity used in this study. Competency ratio is η_0/η_{min}. The grey-scale for the mica fraction given at the bottom corresponds to the grey tones in Figs. 6 and 7.

In our study, it was considered sufficient to use Robin's (1979) model rock, made up of only 'quartz' and 'mica'. Its modal composition can then be described by a single parameter, F, the modal fraction of 'mica'. Its variable creep strength can be represented by a viscosity, η, which varies with F as in Fig. 1(a) (from Robin 1979, fig. 1). Such a curve states, in effect, that a pure-'quartz' rock is competent, presumably because it does not contain the 'micas' which are necessary to catalyse pressure solution; a pure-'mica' rock is also competent, presumably because there is no 'quartz' around and therefore little or no pressure solution; in contrast, rocks of some intermediate composition are relatively weak.

In the absence of any detailed theory or model of how 'micas' might enhance the stress-induced mobilization and transfer of silica, or of models of evolving grain contacts, contact pressures, etc., one cannot propose a

particular, specific form for the curve of Fig. 1(a). For the results presented in this preliminary study we have used a function of the form

$$\eta = \eta_{min}[1 + (C - 1)(F_{min}/F - 1)^2], \qquad (1)$$

represented in Fig. 1(b). F_{min} is the 'mica' fraction for which the viscosity is minimum; η_{min} is that minimum viscosity. C is the *contrast* between the initial viscosity, η_0, of most of the rock, with a 'mica' fraction F_0, and the minimum viscosity, η_{min}; specifically, $C = \eta_0/\eta_{min}$. Equation (1) is such that $F_0 = 0.5F_{min}$. In this study, the parameters are: $C = 100$, $F_{min} = 25\%$, and $F_0 = 12.5\%$ (Fig. 1b).

RHEOLOGY AND FINITE ELEMENT IMPLEMENTATION

Viscous solution

A solution to a viscous flow problem can be obtained by iterating successive stress–strain-increment solutions, each being formally similar to an elastic stress–strain solution (Appendix, equations A2 and A3). Thus the deformation of a rock with a viscosity $\eta = 10^{20}$ Pa s ($= 10^{20}$ kg m^{-1} s^{-1} $= 10^{19}$ poise), over a time interval $\delta t = 10^9$ s (~31.7 years), is equal to the elastic response of a solid with a shear modulus $G = 10^{11}$ Pa (1 Mbar). In the usual modelling of viscous flow, the material is taken to be incompressible. Here, in contrast (see Appendix), the material is allowed to lose or gain volume during deformation, thus simulating pressure solution. In the case when the system is not reinflated (see below), there can only be a loss of volume, that loss being proportional to $p = (\sigma_{xx} + \sigma_{yy})/2$. When the system is reinflated, the silica loss or gain is a linear function of p (see Appendix). In an important paper, Fletcher (1982) has introduced the concept of coupling of viscous flow and diffusional transport, and much of his discussion (particularly pp. 275–280) is relevant to the present contribution.

Numerical implementation

A two-dimensional finite element program, presented by Cheung & Yeo (1979, chapter 2), and using triangular elements (Figs. 2–8), was used as our basic program. A viscous flow solution was obtained by iterating successive stress–strain-increment solutions, each step yielding a strain after a time increment δt. Strains for any single increment must be relatively small in order to yield a proper viscous flow solution. The nodal displacements from one iteration are added to the previous nodal co-ordinates, and the stress–strain solution is solved again for the new positions. The system retains no memory of the previous step.

Cheung & Yeo's (1979) program was modified (1) to implement these iterations and (2) to permit the composition-dependent variations of viscosities. The area, A, of each element is used to calculate its modal fraction, F, and therefore, through equation (1), to calculate its viscosity, η, used in the next iteration. Specifically, if F_0 is the initial 'mica' modal fraction of an element, and A_0 its initial area, its 'mica content' is F_0A_0. Since only 'silica' is mobile, this 'mica content' of an element does not change during deformation. After deformation of an element to area A, its 'mica' modal fraction, used in equation (1), is therefore given by $F = F_0A_0/A$.

Migration of 'silica'

Two end-member possibilities have been modelled: an open system, in which the 'silica' lost by each element is lost from the system, and a closed system, in which the total volume (and thus the total 'silica' content) of the system stays constant while individual elements are free to change.

In the open system, all elements lose volume. As is the case with standard modelling of viscosity, nodal co-ordinates resulting from an iteration are used directly as the input nodal co-ordinates for the next iteration.

The closed system is 'reinflated' at each iteration. This is achieved by calculating the new areas of all elements after the finite element calculation (see Appendix, equation A7). The new area of the system, which is the sum of the areas of all its elements, can be compared with its initial area. All nodal co-ordinates are then expanded by an isotropic dilation to reconstitute that initial area. Thus, elements which enjoy a greater fractional loss of area than the average area loss of the system still lose area, i.e. 'silica', after reinflation, whereas those elements with a lesser fractional area loss than the average prior to reinflation, end up larger, i.e. more 'quartz'-rich than before the iteration.

In his analyses of layer-parallel compression, initial bending and folding, Fletcher (1982) modelled diffusion explicitly, and demonstrated the importance of a characteristic distance $\sqrt{\beta} = \sqrt{2\eta\alpha}$, where α is proportional to the diffusion constant D. In the present work, however, diffusion is only taken into account implicitly. The open system corresponds to a situation in which $\sqrt{\beta}$ is much greater than l, the linear dimension of the system. The closed system can be taken as crudely modelling the case where $\sqrt{\beta}/l \cong 1$.

Finite element grid and initial cleavage seam

We model the development of an isolated seam at the centre of a homogeneous volume of rock, undergoing plane strain. As Fig. 2 shows, the symmetry of the system is such that we only need to model one quarter of it. The grid used consisted of 480 elements loaded along one side. The symmetry of the system was implemented by specifying no x-displacement for one edge and no y-displacement for another (Fig. 2).

The initial cleavage seam nucleus is introduced by assigning to 36 elements a greater initial 'mica' fraction, and therefore a lower viscosity, than those of the rest of the rock. The initial 'mica' fraction, F_{seed}, was F_{seed} =

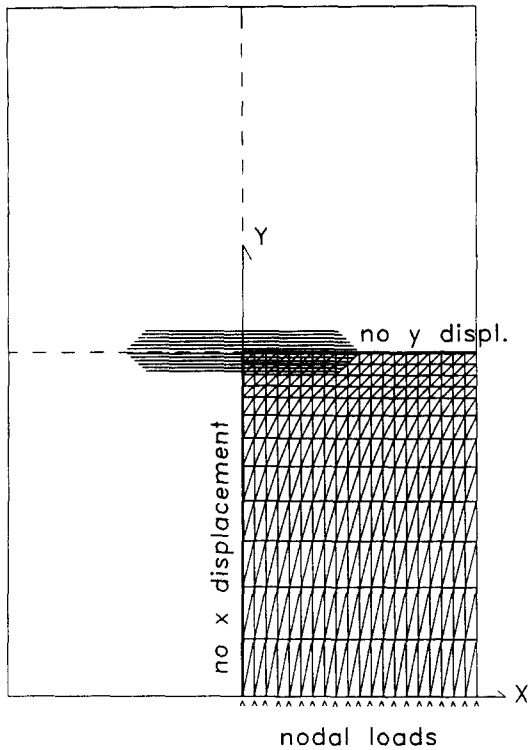

Fig. 2. The finite element grid used is the area made up of triangular elements. The initial cleavage is given by the hatched area.

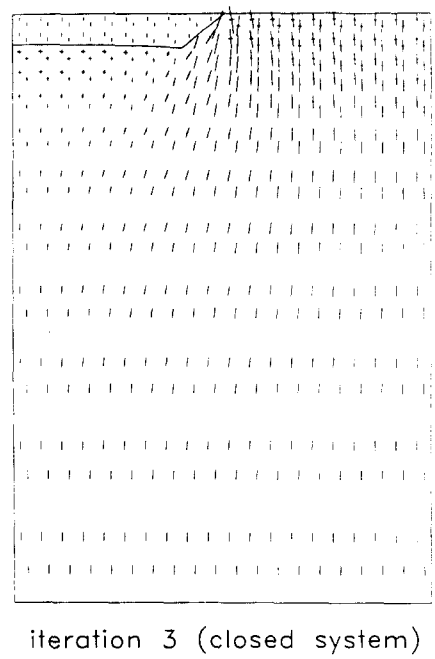

Fig. 3. Principal stresses in 480 elements after three iterations. The lengths of the line segments are scaled proportionally to the magnitudes of the principal compressive stress components.

$0.75F_{min} = 1.5F_0$. For our chosen contrast, $C = 100$, the resulting viscosity of the nucleus was 12% of that of the rest of the rock and equal to 12 η_{min} (Fig. 1b).

The loads were selected such that the strains of all elements in the first iteration were less than 10%. For our arbitrarily selected viscosity of the weakest elements of 10^{18} Pa s, this implies that $\Delta\sigma \times \delta t \leq 10^{17}$ Pa s (i.e. ~1 kbar × 30 years, or 100 bar × 300 years).

RESULTS

Choice of initial parameters

Values for the initial parameters, the contrast C and the initial 'mica' fraction in the cleavage nucleus, F_{seed}, were determined by experiments with the open system. Better results were obtained with a contrast $C = 100$ than with $C = 10$ or 20. A viscosity contrast of 100 is not unrealistic: contrasts of between 1 and 2 orders of magnitude have been used in modelling of folds (Dietrich 1970).

For an initial 'mica' fraction F_{seed} larger than F_0 by only 20%, elements in the open system collapsed before much differentiation had occurred. As the total system loses volume, large viscosity ratios between cleavage seam and matrix need to be established early, before the matrix loses too much strength itself. While such collapse would not occur with a closed system, the same parameters were used for both to allow for comparisons.

Stress distribution around the cleavage seam

The stress distribution among the finite elements is that expected around an anticrack. It is best seen after a few iterations, when the viscosity contrast between the elements ahead of the tip of the cleavage seam and the developing seam itself is at its greatest (Fig. 3). Principal stress trajectories are deflected around the tip of the seam. The seam itself, and the region next to it, on the other hand, are under low relative stress, sheltered by the low strength of the cleavage. Because of the high mean stress in the elements ahead of the tip of the seam, these elements lose the most volume (Fig. 4). The volume loss is, in effect, a loss of 'quartz', and increase in 'mica' fraction, F, and will result in a weakening of the element in the next iteration.

Cleavage evolution

The propagation of the cleavage seam is a direct consequence of the above steps: since the elements ahead of the tip of the cleavage seam are under the highest mean stress, they lose the most 'quartz' and weaken faster than the bulk of the rock. They thus become progressively incorporated into the cleavage.

As elements in the cleavage seam lose more and more 'quartz', their 'mica' concentration brings them on the right-hand side of the curve of Fig. 1, and the seam becomes stronger. Weakened elements at the front of the cleavage tip now cause the stress concentration (Fig. 5). This concentration is not as pronounced as in Fig. 3, because the elements which support it have already become weaker. The source of the stress concentration hence migrates, leaving cleavage behind it and dissolving 'quartz' in front of it. Readers familiar with lattice dislocation motion may note that this propagation of the tip of the cleavage is the continuous equivalent of the climb of an edge lattice dislocation.

The evolution of both closed and open systems (Figs.

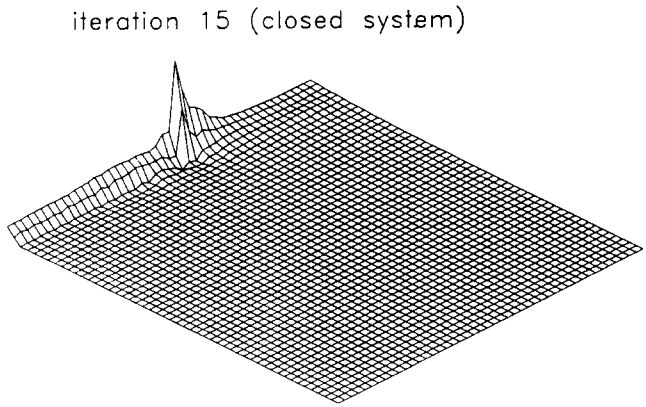

Fig. 4. Surface showing the fractional changes in area of the elements, $\Delta A/A = (\sigma_1 + \sigma_3)/\eta$, after 15th iteration. Peak is at the cleavage tip.

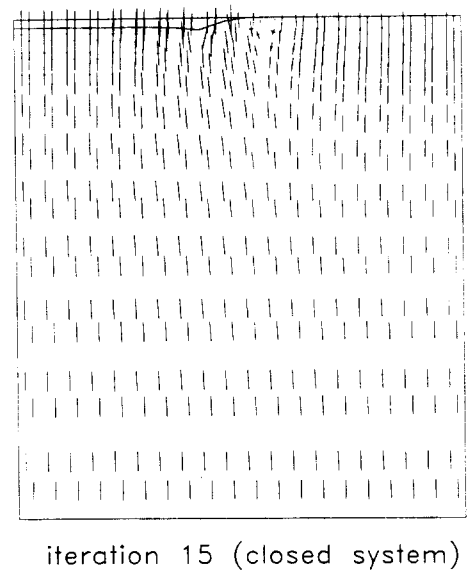

Fig. 5. Principal stresses of elements at 15th iteration. Note how principal stress directions are deflected around elements in front of the original cleavage plane.

6a–g and 7a–c) are discussed in some detail below. In all figures (Figs. 6a–g and 7a–c) the 'mica' fraction is represented by variable grey tones according to the grey scale shown in Fig. 1(b). The overall deformation of the closed and open systems can be seen in Figs. 8(a) & (b). As expected, the constant-volume of the closed system (Fig. 8a) averages to approximately pure shear, whereas the deformation of the open system (Fig. 8b) is best described as a compaction strain.

Evolution of the closed system

At the initial stages of the deformation, the volume of elements within the seam decreases rapidly. At the fifth iteration (Fig. 6b), these elements are already reduced to less than 50% of their original volume. The volume next to the seam is sheltered from the differential stress by the seam, and is consequently less deformed. When the system is reinflated, these elements increase their 'quartz' fraction, and appear as white elements in Fig. 6. As shown in Fig. 1(b), all white elements have less than 12.2% 'mica', compared to their original fraction, F_0, of 12.5%, and have accordingly increased their competency. By the 10th iteration (Fig. 6c) the volume of the cleavage has been reduced further and the number of white elements has increased.

By the 15th iteration (Fig. 6d), a significant increase in the 'mica' fraction has occurred ahead of the original nucleus; in effect, the cleavage has propagated. As more 'silica' is dissolved at, and in front of, the cleavage, which has to be distributed across the system, more elements increase their 'quartz' fraction. The deformation continues by propagating the cleavage further, and by enriching the 'quartz' content of the lithon (Figs. 6e–g).

By the 30th iteration (Fig. 6g), the original nucleus has been reduced to pure 'mica'. The cleavage, defined by elements reduced to less than 50% of their original area, i.e. having more than 25% 'mica', has propagated all the way to the right-hand side; most have in fact more than 40% mica. Outside the cleavage, most elements have gained sufficient 'silica' to dilute their 'mica' fraction to less than 12.2%. Note that the cleavage on the right-hand side is now three-rows wide, i.e. thicker than the original two-row nucleus.

Evolution of the open system

Results of the first iteration (Fig. 7a) are not significantly different from those of the closed system. By the fifth iteration (Fig. 7b), the cleavage seam has a greatly reduced volume, and weakening has occurred in five to six rows in front of it. Since the 'silica' lost by each element is lost from the system, no element can increase its 'quartz' fraction. By the 10th iteration (Fig. 7c), a one-row wide cleavage has propagated half way toward the right-hand-side of the system. All the elements in the system have increased their mica fraction to more than 18%, except for an area adjacent to the cleavage plane. The location of this sheltered area, with a 'mica' fraction of 17%, is the same as that of the 'quartz'-rich areas in Figs. 6(b) & (c). Beyond the 10th iteration, the evolution becomes unrealistic as the 'mica' fraction in the cleavage becomes greater than 1.

CONCLUSION

Our modified finite element modelling, combined with composition-dependent rheology, provides a reasonable description of the development of a cleavage seam. From an initial nucleus with a relatively small departure of its 'mica' fraction from that of the rest of the rock, the seam increased in both its 'mica' fraction and its length. With some differences, this development occurred in both open and closed systems. As one might expect, the cleavage seam grew 'faster' when the dissolved 'silica' left the rock. The results agree in many ways with petrographic observations and expectations.

(1) The stress concentrations around the cleavage plane were as expected from the considerations by

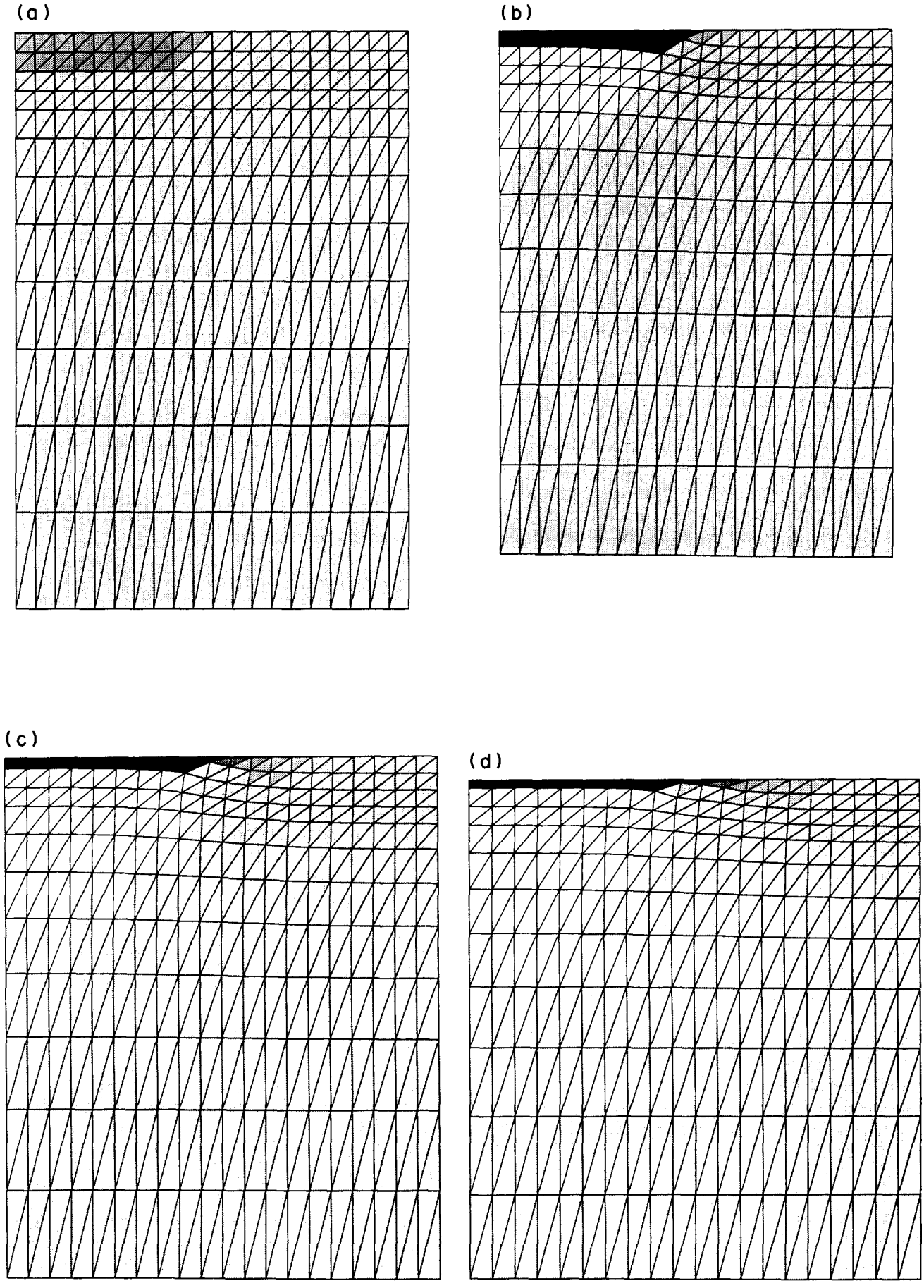

Fig. 6. (a)–(d).

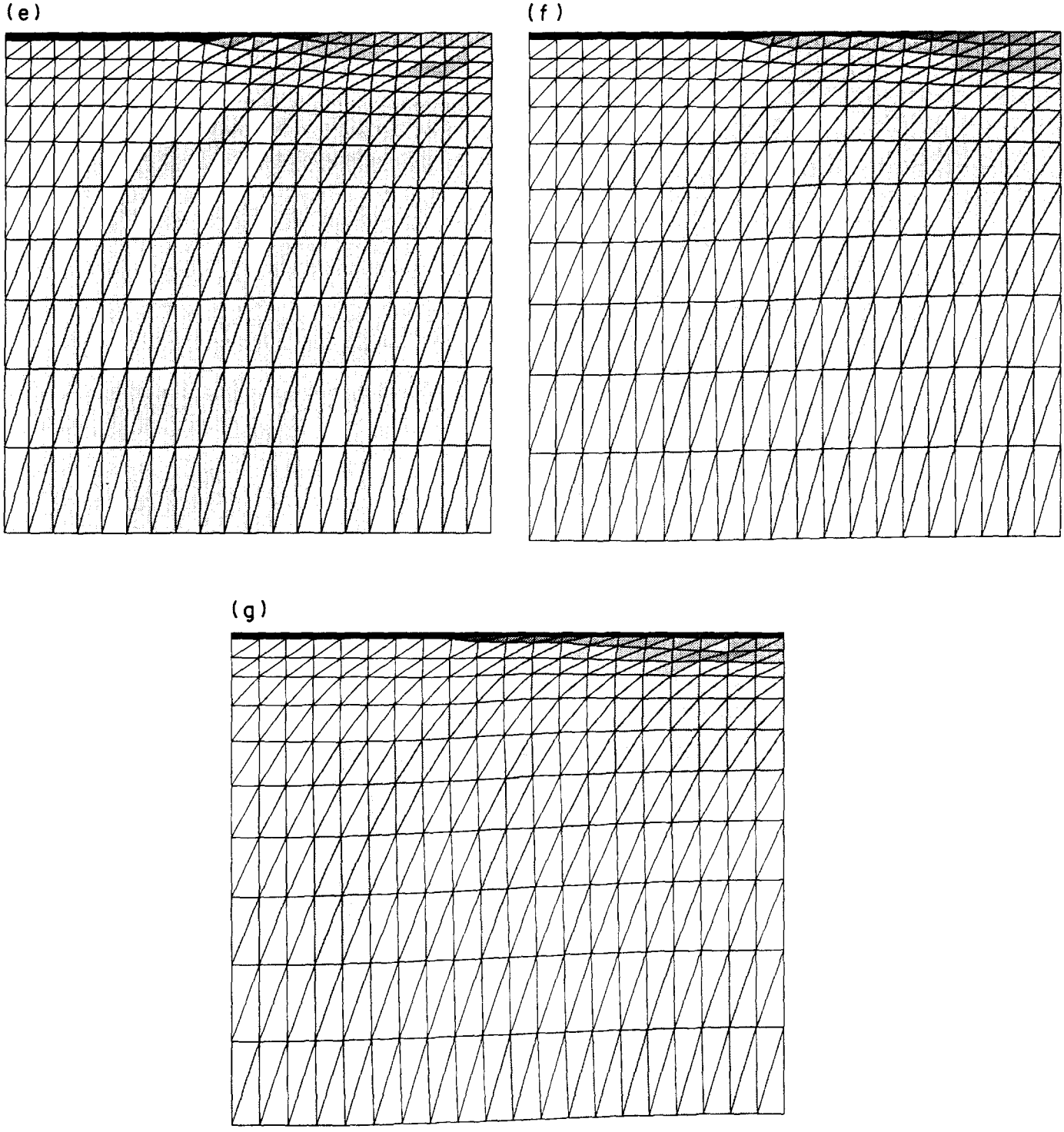

Fig. 6. (e)–(g).

Fig. 6. (a)–(c). Evolution of the closed system. Mica fraction of elements is given by the grey-scale illustrated in Fig. 1. (a) shows iteration 1. (b)–(g) correspond to iterations 5, 10, 15, 20, 25 and 30, respectively.

Fletcher & Pollard (1981). We tentatively interpret the high porosity and the fractures in the 'Process Zone' observed by Raynaud & Carrio-Schaffauser (1992, this issue) to be the result of the stress concentration at the tip of the propagating stylolite–anticrack.

(2) An initial contrast of 100 between the viscosity of most of the rock and the minimum viscosity, η_{min}, were required to cause propagation in both systems. Such contrast is similar to that which leads to realistic-looking folds in the numerical experiments of Dietrich (1970).

(3) The elements immediately adjacent to the most 'mica'-rich elements in the seam became the most 'quartz'-rich in the system, giving a very sharp boundary to the well developed cleavage seam. Sharp boundaries to pressure solution cleavage seams are commonly observed petrographically.

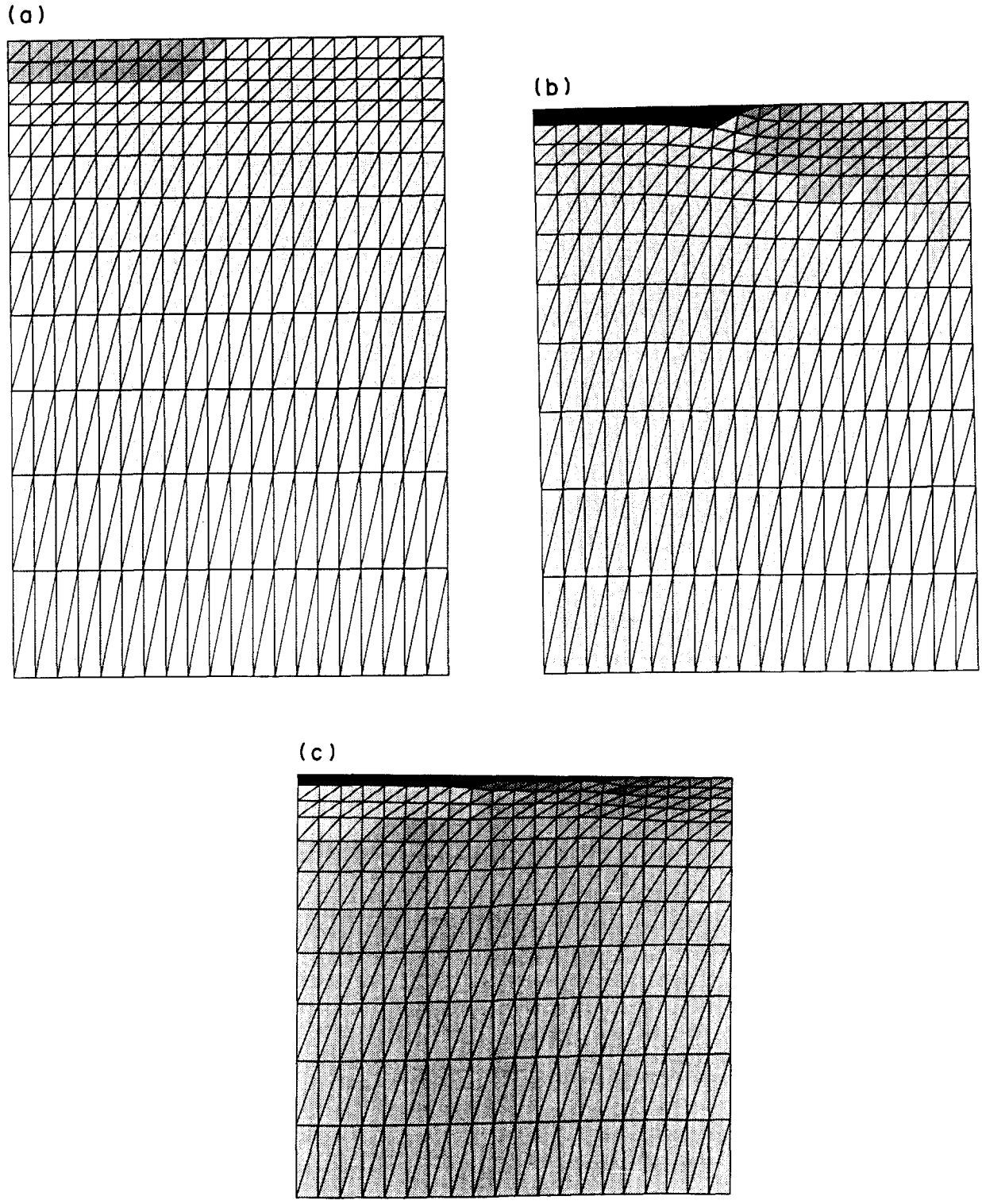

Fig. 7. Evolution of the open system. Mica fraction of elements is given by the grey-scale illustrated in Fig. 1. (a) Shows first iteration ; (b) & (c) correspond to fifth and 10th iterations, respectively.

(4) At the propagating end (right-hand side) of the seam, the zone in which elements lost 'silica' became thicker than the initial nucleus. This is analogous to the petrographic observation that cleavage seams become thicker, and more diffuse, at their terminations.

We consider that these preliminary results have successfully simulated important features of cleavage propagation. This tentative success perhaps justifies the assumptions made in the model and the numerical procedure used. Both composition-dependent viscosity (Fig. 1) and the method used to couple deformation and transfer may enable us to investigate important problems associated with cleavage development. Among such problems which we hope to examine are: the thickening of cleavage seams; the interaction and coalescence of several cleavage seams; their spacing; the formation of Robin's (1979) *equilibrium banding*. A possible shortcoming of the methodology, at the present

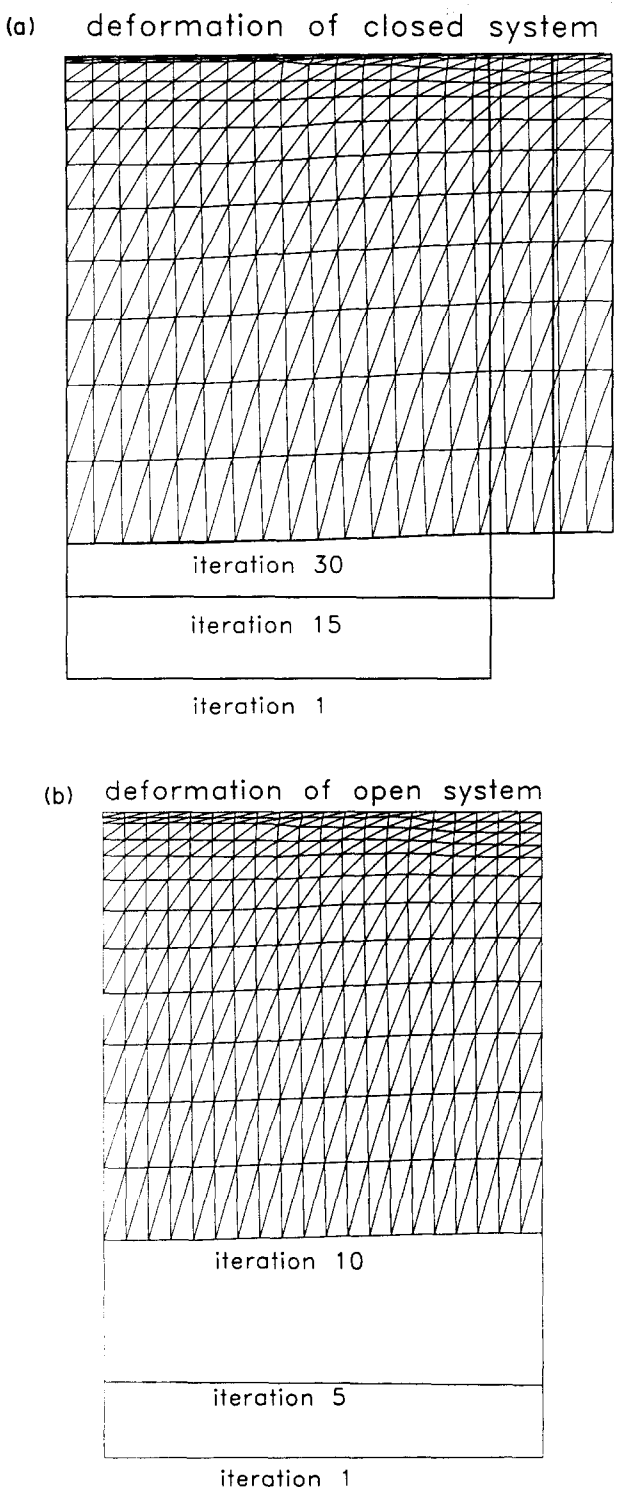

Fig. 8. Overall deformation of systems. (a) Shape of grid of closed system at iterations 1, 15 and 30; (b) shape of grid of open system at iterations 1, 5 and 10.

stage, however, is that it appears to be difficult to simulate diffusion and diffusion range explicitly. Further work is required to try and remedy that.

Acknowledgements—We are grateful to R. M. Stesky for providing suggestions and guidance on the use of the finite element programme, and many discussions in the early stages of the work. Paula MacKinnon was a demanding reader whose comments helped improve earlier versions of the manuscript. The work was supported by National Science and Engineering Research Council of Canada Operating grants to both authors. Help from the computer centers at Brock University and at the University of Toronto, Erindale Campus is gratefully acknowledged.

REFERENCES

Cheung, Y. K. & Yeo, M. F. 1979. *A Practical Introduction to Finite Element Analysis*. Pitman, London.

Dietrich, J. H. 1970. Computer experiments on mechanics of finite amplitude folds. *Can. J. Earth Sci.* **7**, 467–476.

Fletcher, R. C. 1982. Coupling of diffusional mass transport and deformation in a tight rock. *Tectonophysics* **83**, 275–291.

Fletcher, R. C. & Pollard, D. D. 1981. Anticrack model for pressure solution surfaces. *Geology* **9**, 419–424.

Heald, M. T. 1956. Cementation of Simpson and St. Peter sandstone in parts of Oklahoma, Arkansas and Missouri. *J. Geol.* **64**, 16–30.

Jaeger, J. C. 1962. *Elasticity, Fracture and Flow*. Methuen, London.

Raynaud, S. & Carrio-Schaffhauser, E. 1991. Investigation of rock matrix structures in the controlled area of a stylolite. In: *Terra Abs.* (Suppl. 5 to *Terra Nova* **3**, 32).

Raynaud, S. & Carrio-Schaffhauser, E. 1992. Rock matrix structures in a zone influenced by a stylolite. *J. Struct. Geol.* **14**, 973–980.

Robin, P.-Y. F. 1979. Theory of metamorphic segregation and related processes. *Geochim. cosmochim. Acta* **43**, 1587–1600.

Sorby, H. C. 1863. Uber Kalkstein-Geschiebe mit Eindrucken. *Neues Jb. Miner.* **34**, 801–807.

APPENDIX

The analytical and numerical solutions to boundary-value viscous flow problems are commonly solved by using the formalism of elastic rheology, and it is convenient to present the latter. The rheological equation of an isotropically elastic medium deforming in plane strain (e.g. Jaeger, 1962, p. 60, equations 8 and 9) is, in matrix form:

$$\begin{bmatrix}\varepsilon_{xx}\\ \varepsilon_{yy}\\ \varepsilon_{xy}\end{bmatrix}=\frac{1+\nu}{E}\begin{bmatrix}1-\nu & -\nu & 0\\ -\nu & 1-\nu & 0\\ 0 & 0 & 1\end{bmatrix}\begin{bmatrix}\sigma_{xx}\\ \sigma_{yy}\\ \sigma_{xy}\end{bmatrix}, \tag{A1}$$

where E is Young's modulus and ν is Poisson's ratio. If the elastic material is incompressible, i.e. $\nu = 0.5$, the rheological equation reduces to

$$\begin{bmatrix}\varepsilon_{xx}\\ \varepsilon_{yy}\\ \varepsilon_{xy}\end{bmatrix}=\frac{3}{4E}\begin{bmatrix}1 & -1 & 0\\ -1 & 1 & 0\\ 0 & 0 & 2\end{bmatrix}\begin{bmatrix}\sigma_{xx}\\ \sigma_{yy}\\ \sigma_{xy}\end{bmatrix}. \tag{A2}$$

We note that in this special case of an incompressible material, the determinant of the 3×3 elasticity matrix is zero: the matrix can therefore not be inverted. This means that one cannot uniquely determine the components of stress, specifically σ_{xx} and σ_{yy}, from the components of strain. Only their difference, $\sigma_{xx} - \sigma_{yy}$, is unique; their actual values are commonly given in terms of the 'floating' parameter, $p = -(\sigma_{xx} + \sigma_{yy})/2$. Because of that non-uniqueness, incompressible materials commonly give difficulties in finite element programs, including in the program used in this work.

The strain increment of an incompressible Newtonian viscous material deforming in plane strain during a time interval δt is similarly given by:

$$\begin{bmatrix}\delta\varepsilon_{xx}\\ \delta\varepsilon_{yy}\\ \delta\varepsilon_{xy}\end{bmatrix}=\frac{1}{4\eta}\begin{bmatrix}1 & -1 & 0\\ -1 & 1 & 0\\ 0 & 0 & 2\end{bmatrix}\begin{bmatrix}\sigma_{xx}\\ \sigma_{yy}\\ \sigma_{xy}\end{bmatrix}. \tag{A3}$$

As is the case for the elastic strain of an incompressible material, and for the same reason, this relation cannot be inverted to give unique stress components from the strain. The components of stress are therefore generally given in terms of the 'floating' pressure, p (see e.g. Jaeger, 1962, p. 71, equations 11 and 12):

$$\begin{aligned}\sigma_{xx} + p &= 2\eta\varepsilon_{xx}\\ \sigma_{yy} + p &= 2\eta\varepsilon_{yy}\\ \sigma_{xy} &= 2\eta\varepsilon_{xy}.\end{aligned} \tag{A4}$$

In the present work, by contrast, the possible loss or gain of silica by a volume of rock make it eminently compressible. If an elastic material has a Poisson's ratio of 0, its elastic strain is

$$\begin{bmatrix}\varepsilon_{xx}\\ \varepsilon_{yy}\\ \varepsilon_{xy}\end{bmatrix}=\frac{1}{E}\begin{bmatrix}1 & 0 & 0\\ 0 & 1 & 0\\ 0 & 0 & 1\end{bmatrix}\begin{bmatrix}\sigma_{xx}\\ \sigma_{yy}\\ \sigma_{xy}\end{bmatrix}. \tag{A5}$$

Analogously, in the viscous material modelled here, the strain increment during a time interval δt is, prior to any eventual reinflation,

$$\begin{bmatrix} \delta\varepsilon_{xx} \\ \delta\varepsilon_{yy} \\ \delta\varepsilon_{xy} \end{bmatrix} = \frac{1}{\eta} \begin{bmatrix} 1 & 0 & 0 \\ 0 & 1 & 0 \\ 0 & 0 & 1 \end{bmatrix} \begin{bmatrix} \sigma_{xx} \\ \sigma_{yy} \\ \sigma_{xy} \end{bmatrix}. \tag{A6}$$

In the case of an open system, the volume lost during δt is therefore

$$\delta\varepsilon_{xx} + \delta\varepsilon_{yy} = (\sigma_{xx} + \sigma_{yy})/\eta = -2p/\eta.$$

In the case of the closed system, a uniform isotropic strain is added everywhere to reinflate that system, and the total strain over the time interval δt represented by one iteration is

$$\begin{bmatrix} \delta\varepsilon_{xx} \\ \delta\varepsilon_{yy} \\ \delta\varepsilon_{xy} \end{bmatrix} = \frac{1}{\eta} \begin{bmatrix} 1 & 0 & 0 \\ 0 & 1 & 0 \\ 0 & 0 & 1 \end{bmatrix} \begin{bmatrix} \sigma_{xx} \\ \sigma_{yy} \\ \sigma_{xy} \end{bmatrix} + \begin{bmatrix} \delta\varepsilon' \\ \delta\varepsilon' \\ 0 \end{bmatrix}. \tag{A7}$$

As explained in the main text, the isotropic reinflation strain, $\delta\varepsilon'$, is such that the total area of the system is reestablished to its value prior to the finite element calculation.